Microporous and Mesoporous Materials 136 (2010) 92–96

Contents lists available at ScienceDirect

Microporous and Mesoporous Materials

journal homepage: www.elsevier.com/locate/micromeso

Changes in the medium-range order of zeolite A by mechanical and thermal amorphization

Toru Wakihara [a,*], Kaku Sato [a], Shinji Kohara [b], Gopinathan Sankar [c], Junichi Tatami [a], Katsutoshi Komeya [a], Takeshi Meguro [a], Kenneth J.D. MacKenzie [d]

[a] Graduate School of Environmental and Information Sciences, Yokohama National University, 79-7 Tokiwadai, Hodogayaku, Yokohama 240-8501, Japan
[b] Japan Synchrotron Radiation Research Institute, Mikazuki, Sayo, Hyogo 679-5198, Japan
[c] Department of Chemistry, University College London, 20 Gordon Street, London WC1H 0AJ, UK
[d] School of Chemical and Physical Sciences, Victoria University of Wellington, P.O. Box 600, Wellington 6140, New Zealand

ARTICLE INFO

Article history:
Received 13 April 2010
Received in revised form 29 July 2010
Accepted 2 August 2010
Available online 7 August 2010

Keywords:
Ring
Amorphization
Medium-range order
Zeolite A

ABSTRACT

Crystalline zeolite A was amorphized by mechanical and thermal treatments, and the resulting changes in the atomic arrangement are characterized by HEXRD, ^{27}Al MAS NMR and Raman spectroscopy. HEXRD measurements revealed that the 6R and 8R rings are distorted and/or destroyed, while the 4R ring is preserved during mechanical treatment, but all rings are distorted and/or destroyed by thermal treatment. Data from ^{27}Al MAS NMR and Raman spectroscopy also support these results. Furthermore, recrystallization behavior is found to be different between mechanically and thermally amorphized solids.

1. Introduction

Zeolites have been used as ion exchangers, adsorbents, catalysts, molecular-sieving membranes and for many other uses [1–3]. Thus, it is important to understand the structural changes involved during amorphization as a result of mechanical and thermal stresses. For example, understanding the amorphization of zeolite is crucial for control of the petroleum refinery process since the destruction of the zeolite structure often occurs under conditions of high temperature and steam. Changes in the crystallinity and pore structures can be estimated by X-ray diffraction, N_2 adsorption and catalytic reactions, among other methods [4–7]. However, it is difficult to understand the amorphization of zeolites on an atomic scale because of their disordered nature. Although the local structure of disordered materials may be determined by NMR [8,9] or EXAFS [10] techniques, the structural information obtained by these methods is not sufficient to determine the nature of the ring structures over medium-range distances. Diffraction methods (either X-ray or neutron) are commonly used to obtain the atomic arrangement of disordered materials [11,12]. To analyze the structure of disordered materials, it is necessary to obtain the range structure factor $S(Q)$ in a wide scattering vector Q ($Q = 4\pi \sin\theta/\lambda$, θ: scattering angle, λ: wavelength of photons or neutrons), since the resolution in real space depends on the Q_{max} of the Fourier transformation of $S(Q)$. It is essential, therefore, to conduct measurements at high energies (i.e. very short wavelengths ca. 0.2 Å), which is now possible using third generation synchrotron radiation sources. Although neutron diffraction is a valuable technique to obtain similar information, it is sensitive to O–O correlations and small amounts of hydrogen introduce large uncertainties during data normalization [13]. X-ray diffraction is sensitive to Si–Si(Al) correlations, which are more important in determining the medium-range order of zeolites and related materials [14–17].

Zeolite A, one of the most representative zeolites, is the focus of this study. Fig. 1 shows the structure of zeolite A from a single crystal structure determination. The zeolite A framework consists of 4-membered and 6-membered rings (4R and 6R) assembled in three dimensions to produce larger units such as 8-membered rings (8R), double 4-membered rings (D4R) and sodalite cages. The distribution of the rings in zeolite A is also shown in Fig. 1. These basic units are seen in many zeolite structures such as faujasite and sodalite. Fig. 1 also shows distances from a Si(Al) to the second nearest oxygen atom in zeolite A. This distance in 4R is ca. 3.9 Å, and this is shorter than the comparable distances in 6R and 8R. By characterizing the medium-range order of crystalline and amorphized zeolite, we hope to understand the transitions from the crystalline to the amorphous state. Recently, medium-range orders of amorphized zeolites under high pressure have been

---

[*] Corresponding author. Tel./fax: +81 45 339 3957.
E-mail address: wakihara@ynu.ac.jp (T. Wakihara).

1387-1811/$ - see front matter © 2010 Elsevier Inc. All rights reserved.
doi:10.1016/j.micromeso.2010.08.002

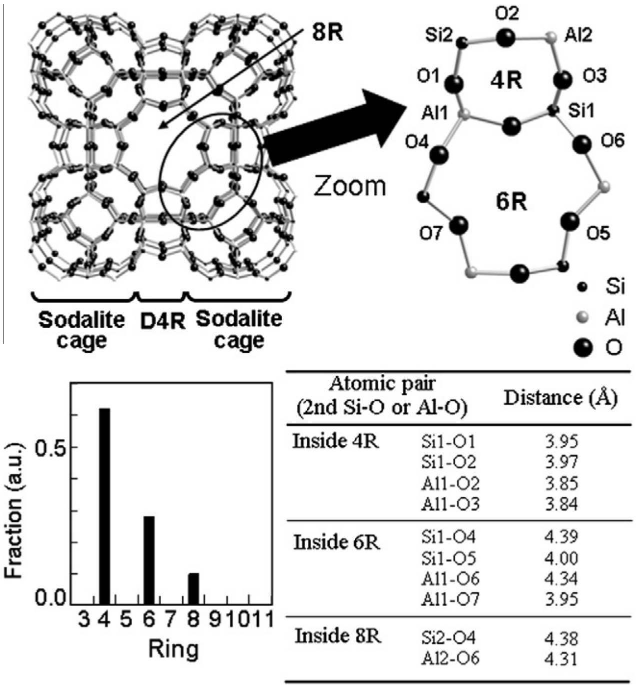

Atomic pair (2nd Si-O or Al-O)		Distance (Å)
Inside 4R	Si1-O1	3.95
	Si1-O2	3.97
	Al1-O2	3.85
	Al1-O3	3.84
Inside 6R	Si1-O4	4.39
	Si1-O5	4.00
	Al1-O6	4.34
	Al1-O7	3.95
Inside 8R	Si2-O4	4.38
	Al2-O6	4.31

Fig. 1. Top left: the crystal structure of zeolite A. Top right: the typical shape of the ring structures present in the three-dimensional configurations. Bottom left: the ring distribution of zeolite A. Bottom right: table containing the distances of 2nd Si–O and Al–O.

investigated; the position of the X-ray diffraction peaks and the pair distribution functions have been analyzed [18,19]. However, there are few reports on other amorphization processes, such as mechanical and thermal amorphization. In this study, crystalline zeolite A was amorphized by mechanical or thermal treatments, and the transition from the crystalline to the amorphous states characterized by HEXRD, ^{27}Al solid-state nuclear magnetic resonance with magic angle spinning (^{27}Al MAS NMR) and Raman spectroscopy.

2. Experimental

2.1. Sample preparation

Commercial zeolite A (LTA type zeolite: 4A, Si/Al = 1, Cation: Na, Tosoh Co., Japan) was used in this study. First, the sodium ions present in zeolite were exchanged with ammonium ions using a conventional method. Briefly, approximately 30 g of the zeolite was added to 300 ml of 10 wt.% ammonium nitrate (NH_4NO_3, Wako Pure Chemical Industries Ltd.) solution at 80 °C and stirred for 24 h. The slurry was then centrifuged and the supernatant liquid was decanted off. The residual solid was washed with distilled water several times. The solids were then retreated with fresh solution of ammonium nitrate in a similar manner. This process was repeated four times in total. Finally, the ion-exchanged zeolites were filtered and dried. The composition of the product was confirmed by X-ray fluorescence (XRF, JSX-3202, JEOL) and no sodium was detected, indicating that the empirical formula of the product was NH_4SiAlO_4.

The ion-exchanged zeolite A was amorphized by mechanical or thermal treatment. First, the ion-exchanged zeolite A was allowed to be amorphized through the milling using a planetary ball mill (P6-type, Fritsch) equipped with a silicon nitride pot and balls. The milling was conducted for two 15-min periods with a 15-min break between them to avoid overheating the samples. The material was ground at 500 rpm for 15, 30 or 90 min, and designated as MA15, MA30 or MA90, respectively (MA: mechanical amorphization). The ion-exchanged zeolite A was also amorphized by the thermal treatment. The ion-exchanged zeolite A was weighed into an alumina boat (0.5 g), placed in an electric furnace fitted with a high-purity alumina work tube, and heated to 500 °C at a rate of 5 °C/min in Ar gas (99.999% purity) for 2 h; this was designated as TA (thermal amorphization).

2.2. Characterization

The phases present in the products were identified by conventional X-ray diffractometry (XRD: RINT2500, Rigaku, Tokyo, Japan) using CuKα radiation operated at 50 kV and 300 mA. For HEXRD measurement, 200 mg of the sample was pressed into a disc and the measurements carried out at room temperature. HEXRD experiments were carried out on the horizontal two-axis diffractometer, optimized for structural measurements in glass and liquid, and built at the BL04B2 high-energy monochromatic bending magnet beam line of SPring-8, which operates at 8 GeV. A bent Si(2 2 0) crystal mounted on the monochromator stage, fixed at a Bragg angle of 3° in the horizontal plane, provided incident photons at 61.63 keV (wavelength: 0.2012 Å). $Q_{\max}$ collected in this study was ca. 25 Å^{-1}. The collected data were subjected to well-established analysis procedures, such as absorption, background and Compton scattering corrections, and then normalized to Faber–Ziman [20] total structure factor $S(Q)$. These corrected data were used to calculate the total correlation function $T(r)$ using the function

$$T(r) = 4\pi\rho r + \frac{2}{\pi}\int_{Q_{\min}}^{Q_{\max}} Q[S(Q)-1]\sin(Qr)dQ + 1 \tag{1}$$

where ρ is the atomic number of density [21].

The ^{27}Al MAS NMR spectra were obtained at 11.7 T using a Bruker AMX 500 (Rheinstetten, Germany) and a Varian Unity 500 spectrometer (Palo Alto, CA) at a frequency of 130.3 MHz. A Doty high-speed MAS probe was used, at 12.2 kHz and using a 1-ms, 15° pulse with a recycle time of 1 s. The ^{27}Al chemical shifts were measured with respect to a 1 M aqueous $AlCl_3$ solution. Products were also characterized by Raman spectroscopy (JASCO NRS-2000). The wavelength of the laser was 514 nm and laser power approximately 5–10 mW.

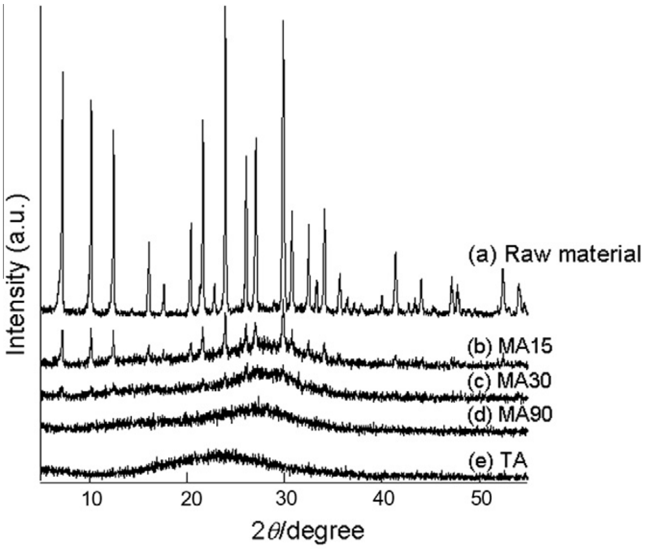

Fig. 2. XRD patterns of the samples: (a) raw material, (b–d) MA15, 30 and 90, respectively, (e) TA. All Bragg peaks seen in the samples are due to zeolite A.